The Structure of Membrane Crystals of the Light-harvesting Chlorophyll *a/b* Protein Complex

W. KÜHLBRANDT*‡, TH. THALER*, and E. WEHRLI*
**Institut für Zellbiologie, ETH-Hönggerberg, CH-8093 Zürich, Switzerland; and ‡Institut für Kommunikationstechnik, Abt. Bildwissenschaften, ETH Zentrum, CH-8092 Zürich, Switzerland*

ABSTRACT Membrane crystals of the light-harvesting chlorophyll *a/b* protein complex from pea chloroplasts were investigated using electron microscopy and image analysis. The membrane crystals formed upon precipitation of the detergent-solubilized complex with mono- and divalent cations in the presence of small amounts of Triton X-100. The crystalline fraction contained two polypeptides of 25,000 and 27,000 mol wt. Freeze-dried and freeze-etched specimens showed a periodic honeycomb structure on the surface of membrane crystals. Double replicas of freeze-fractured sheets showed a hexagonal lattice of particles on both fracture faces. Image analysis of negatively stained membrane crystals suggested that they had threefold rather than sixfold symmetry in projection. A projection map at 20-Å resolution revealed two triangular structural units of opposite handedness per crystallographic unit cell. The structural units appeared to be inserted bidirectionally into the membrane, alternating in orientation perpendicular to the membrane plane.

Photosynthetic membranes of higher plants and green algae contain large amounts of a chlorophyll *a/b* protein complex that harvests solar energy (for reviews see references 1–4). The light-harvesting complex (LHC) occurs mainly in the thylakoid stacks of chloroplast grana where it appears to be associated with the chlorophyll-protein complexes of photosystem II (1, 5). Native LHC probably exists as an oligomer of identical subunits (6, 7). The complex spans the thylakoid membrane, exposing different antigenic sites on the two surfaces (8). LHC isolated from green algae (9), spinach (7, 8, 11), barley (10, 11, 18), and pea leaves (7, 11–16) contains one or two main polypeptides of 21,000–29,000 mol wt, each binding an equal number of three to six molecules of chlorophyll *a* and *b* (3). The two polypeptides of pea LHC appear to be phosphorylated (15) and may be structurally related (16).

LHC can be isolated from chloroplasts by treatment with nonionic detergents and gradient centrifugation (12). The isolated complex precipitates from solution upon addition of mono- and divalent cations, forming membrane crystals that tend to aggregate into stacks (13, 14, 17, 18). The stacking of crystalline sheets in vitro is analogous to the process of grana formation in vivo, which is also cation-controlled (19, 20). LHC thus appears to have a dual function as an antenna complex and as a factor mediating membrane adhesion. The structure of crystalline arrays of LHC has previously been studied by electron microscopy (14, 18, 21) and x-ray diffraction of oriented pellets (21). Simpson (18) observed that freeze-fractured precipitates of barley LHC contained hexagonal arrays of 70–90-Å particles with a repeat distance of 122 Å. McDonnel and Staehelin (14) also described hexagonal arrays of 80-Å particles with a center-to-center distance of 118 Å in fracture faces of pea LHC incorporated into lipid vesicles. Li and Hollingshead (21) reported two types of lattices in crystalline precipitates of pea LHC. One type that formed in the absence of lipid was apparently a hexagonally close-packed array of the complex with 85-Å repeat distance and poor long range order. The other type, which appeared to be identical to the regular arrays previously described, formed in the presence of lipid and had a 125-Å unit cell. On the basis of low resolution diffraction data, Li and Hollingshead proposed that the membrane crystals belonged to the P622 space group.

We investigated the composition, structure, and symmetry of pea LHC membrane crystals that formed under controlled ionic conditions in the presence of low concentrations of the detergent, Triton X-100. These arrays had a repeat distance of 125 Å and showed a particularly high degree of order. Various electron microscopic and image processing techniques revealed the structure of membrane crystals. The structural unit of the complex appeared to have threefold symmetry, resembling, in projection, an equilateral triangle. The symmetry of membrane crystals indicated that they belonged to the P321 space group. Both the P321 space group found by us, and the P622 space

THE JOURNAL OF CELL BIOLOGY · VOLUME 96 MAY 1983 1414–1424

group suggested by Li and Hollingshead imply bidirectional insertion of the complex into the membrane crystal. However in P321 the complex itself is asymmetrical with respect to the membrane.

MATERIALS AND METHODS

Isolation and Crystallization of LHC: Peas (*Pisum sativum* var. carnosa cv. Sugar Snap) were grown in a standard hydroculture medium (Perlit substrate moistened with half-strength Hoagland mineral solution). A 16-h photoperiod was maintained with fluorescent and incandescent light of 13,000-lx intensity (68 W/m^2). Leaves of 2-wk-old plants were harvested. LHC was isolated as described by Burke et al. (12) with minor modifications. The chloroplasts were osmotically shocked in 1 mM Tricine, 10 mM NaCl, and 5 mM EDTA (pH 7.8) before washing in 5 mM EDTA and 0.1 M sorbitol (pH 7.8). The LHC fraction was separated on sucrose density gradients containing 0.05% (wt/vol) Triton X-100 (13). Spectra recorded during and after the isolation procedure indicated that photo-oxidation of LHC did not occur.

The complex formed crystalline precipitates upon addition of $MgCl_2$ and KCl (12). Thin, well-ordered membrane crystals were obtained by dialysis of the density gradient fraction against 18 mM sodium cacodylate, pH 6.8, 0.1% (wt/vol) Triton X-100, 10 mM $MgCl_2$, and 200 mM KCl.

Biochemical Characterization: Chlorophyll-protein complexes were separated on sodium dodecyl sulfate (SDS) polyacrylamide tube gels according to Anderson et al. (22) using an SDS/chlorophyll ratio of 7.5:1 (wt/wt) (23). The chlorophyll distribution was determined by scanning unstained gels in a Beckman DB spectrophotometer (Beckman Instruments, Inc., Fullerton, CA). Tube gels were re-electrophoresed on SDS polyacrylamide slab gels.

Standard SDS polyacrylamide gel electrophoresis was carried out as described by Takács (24). Precipitated LHC was solubilized in 62.5 mM Tris-HCl sample buffer pH 6.8, containing 10% (vol/vol) glycerol, 5% (vol/vol) 2-mercaptoethanol, 2.3% (wt/vol) SDS, and 0.01% bromophenolblue. The samples were either heated to 100°C for 3 min or loaded without prior incubation on a 15% polyacrylamide gel. Gels were stained in 0.25% Coomassie Brilliant Blue R 250 in methanol/acetic acid/H_2O at a volume ratio of 5:1:5. After destaining, SDS gels were silver stained according to Wray et al. (25) to detect minor components.

Chlorophyll concentrations and chlorophyll *a/b* ratios were determined in 80% acetone (26). Protein was measured according to the method of Lowry et al. (27) using SDS to eliminate interference of Triton X-100 (28).

Preparation of Specimens for Electron Microscopy: Suspensions of crystalline LHC were pelleted through a 0.5-M sucrose cushion and dialyzed against 10-mM Tricine buffer (pH 7.8). Resuspended pellets were freeze-fractured and freeze-etched in a Balzers BAF 300 apparatus (Balzers-Union, Inc., Balzers, Liechtenstein). A 400-mesh gold specimen support grid was sandwiched with some suspension between two thin copper platelets and frozen in liquid propane at −190°C. The copper platelets were inserted into a hinge-fracturing device and fractured at −120°C. Other specimens were fractured at −100°C and etched for 60 s. A 20-Å film of platinum-carbon was evaporated onto the specimen at a 45° angle, followed by a 150-Å carbon film at a 90° angle. Double replicas were obtained using a pair of gold finder grids instead of a single gold grid (29).

Crystalline sheets of LHC adsorbed to glow discharged, and carbon-coated specimen support grids were washed on a drop of distilled water, frozen in liquid nitrogen, dried at −80°C at 10^{-6} torr, and shadowed as described above. Other specimens were negatively stained with two changes of a 2% uranyl acetate solution after washing with distilled water.

Blocks for sectioning of crystalline precipitates were prepared by the freeze-substitution method (30) to avoid material loss. Sections were cut with a diamond knife on an LKB ultramicrotome (LKB Produkter, Brommer, Sweden) and stained with lead citrate.

Electron Microscopy: Electron micrographs were taken at an acceleration voltage of 100 kV in a JEOL 100 C electron microscope equipped with a side-entry goniometer stage and a minimal dose attachment. Images were recorded on Agfa Scientia film (Agfa-Gevaert, Leverkusen, Germany) at ~5,000 Å underfocus. Micrographs used for image analysis were taken, minimizing the specimen irradiation. Sheets were located and positioned at low magnification and recorded at × 33,000. The estimated total electron dose per micrograph was 10–15 e/Å^2. The instrument magnification was calibrated with catalase as a standard.

Image Analysis: Areas of good crystalline order on recorded images were selected on a surveying laser diffractometer and densitometered on a Optronix P 1700 photoscan/photowrite unit (Optronix International Inc., Chelmsford, MA). Square arrays of 512 × 512 steps were digitized with a stepsize and aperture of 25 μm, corresponding to 7.6 Å at the specimen. Fourier transforms of the densitometered areas were calculated on a CDC Cyber 722 computer (Cyber Systems, Anaheim, CA) using a fast Fourier transform routine by O. Kübler (Institut für Kommunikationstechnik). Micrographs of metal-shadowed specimens were computer-processed using programs by O. Kübler that combined amplitudes and phases at lattice points to generate noise-filtered images. A detailed analysis of reflexion amplitudes and phases was carried out for micrographs of negatively stained membrane crystals. Amplitudes and phases of reflexions above background level were collected at reciprocal lattice points and symmetrized for P6 and P3 symmetry. A contour map of the structure in projection was calculated from averaged phases and amplitudes. Other contour maps were calculated from symmetrized and unsymmetrized data derived from individual images.

RESULTS

Isolation and Biochemical Characterization of LHC

The LHC fraction isolated from Triton X-100 solubilized membranes showed the intense red fluorescence characteristic of the antenna complex. A high chlorophyll *a/b* ratio of 1.8 indicated that contaminating chlorophyll *a*-binding components were present. Precipitation of the gradient fraction with $MgCl_2$ and KCl yielded highly purified microcrystalline LHC with a chlorophyll *a/b* ratio ~1.1.

Thylakoid membranes and Triton X-100 solubilized, unprecipitated LHC were electrophoresed on SDS polyacrylamide tube gels under conditions that left the protein-chlorophyll complexes largely undissociated (10). Unstained gels of whole thylakoids (Fig. 1 *a*) showed the characteristic bands of photosystem I and II, and two main bands that represented the antenna complexes, referred to as LHCP[1] and LHCP[3] (22). Unstained gels of isolated LHC (Fig. 1 *b*) showed the LHCP[1] and LHCP[3] bands, and some free pigment.

Standard SDS polyacrylamide gel electrophoresis of the purified complex showed two polypeptide bands migrating at apparent molecular weights of 25,000 and 27,000 (Fig. 1 *c*).

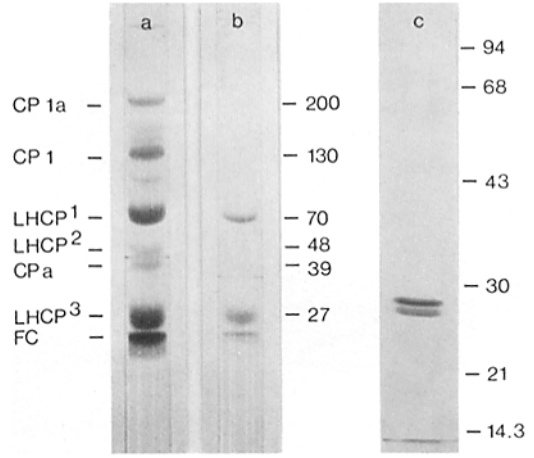

FIGURE 1 SDS polyacrylamide tube gels of pea thylakoids (*a*), and the isolated LHC fraction (*b*), run under conditions that leave the chlorophyll-protein complexes largely undissociated (see Materials and Methods). The nomenclature is that used by Anderson et al. (23), who also determined the apparent molecular weights shown here. The actual molecular weights of chlorophyll-protein complexes may be considerably higher (1). *CP Ia* and *CP I* are components of photosystem I. *CP a* represents the reaction center complex of photosystem II (22). The purified LHC fraction contains only the *LHCP*[1] and *LHCP*[3] bands and some free chlorophyll (*FC*). Re-electrophoresis of the two main LHC bands showed that *LHCP*[1] is an oligomer of *LHCP*[3]. (*c*) SDS polyacrylamide slab gel of crystalline LHC. Two polypeptides of 25,000 and 27,000 apparent mol wt are resolved. The positions of marker polypeptides (with molecular weights in kdaltons) are indicated.

Usually, the upper band appeared more intense in Coomassie Brilliant Blue staining, but both polypeptides were main components. No minor components were detected by the highly sensitive silver-staining method. Upon re-electrophoresis on SDS gels, both components migrated as a single band (not shown), demonstrating that they represented different polypeptides rather than different electrophoretic forms of the same protein. Re-electrophoresis of the $LHCP^1$ and $LHCP^3$ band (Fig. 1*a*) on SDS slab gels (not shown) indicated that both complexes contained the 25,000 and 27,000-mol wt·polypeptides.

Structural Characterization of Crystalline Sheets

Electron microscopy of freeze-dried, platinum-carbon-shadowed precipitates revealed thin crystalline sheets (Fig. 2) with a regular surface structure. The thickness measured from the shadow length at the edge of the thinnest sheets was 40–60 Å, indicating that these sheets were single layers. The membrane surface exhibited a regular array of roughly circular depressions or holes with a repeat distance of ~125 Å.

A different type of periodic structure was found on the two complementary fracture faces of freeze-fractured membrane crystals (Fig. 3). Both faces showed apparently identical hexagonal arrays of particles with a repeat distance of 125 Å. No other regular structure was observed on fracture faces, but small featureless patches were found occasionally.

The periodic structures on the membrane surfaces and fracture faces occurred side-by-side, on the same crystalline sheet, in freeze-etched preparations (Fig. 4). The transition from one structure type to the other was marked by a step of less than the thickness of a membrane crystal, indicating that part of the top half-membrane had come off, exposing the fracture face. The structure on the membrane surface, not observed in unetched preparations, was exposed by sublimation of ice surrounding the membrane crystals.

Computer filtered images (Fig. 5) clearly showed the detail on the membrane surfaces and fracture faces. Reflexions out to the (4,0), corresponding to a resolution of ~30 Å, were visible in the laser diffractometer and used to generate the filtered images. The structure on the membrane surface, revealed by processing images of freeze-dried and freeze-etched, unidirectionally shadowed preparations, showed a hexagonal pattern of roughly triangular units. The triangular units were arranged around roughly circular depressions in the membrane surface that measured 90–100 Å diam (Fig. 5, *a* and *b*). The crystallographic unit cell appeared to contain two such triangular elements that were in contact at their apexes. At the attained resolution of ~30 Å, we were unable to distinguish two structure types that might correspond to the two membrane surfaces. In the case of freeze-dried specimens, this could be due to preferential adsorption of one side to the carbon film, but such an effect can be ruled out for freeze-etched preparations. Both sides of the membrane therefore seemed to be structurally identical.

Computer-processed images of complementary fracture faces

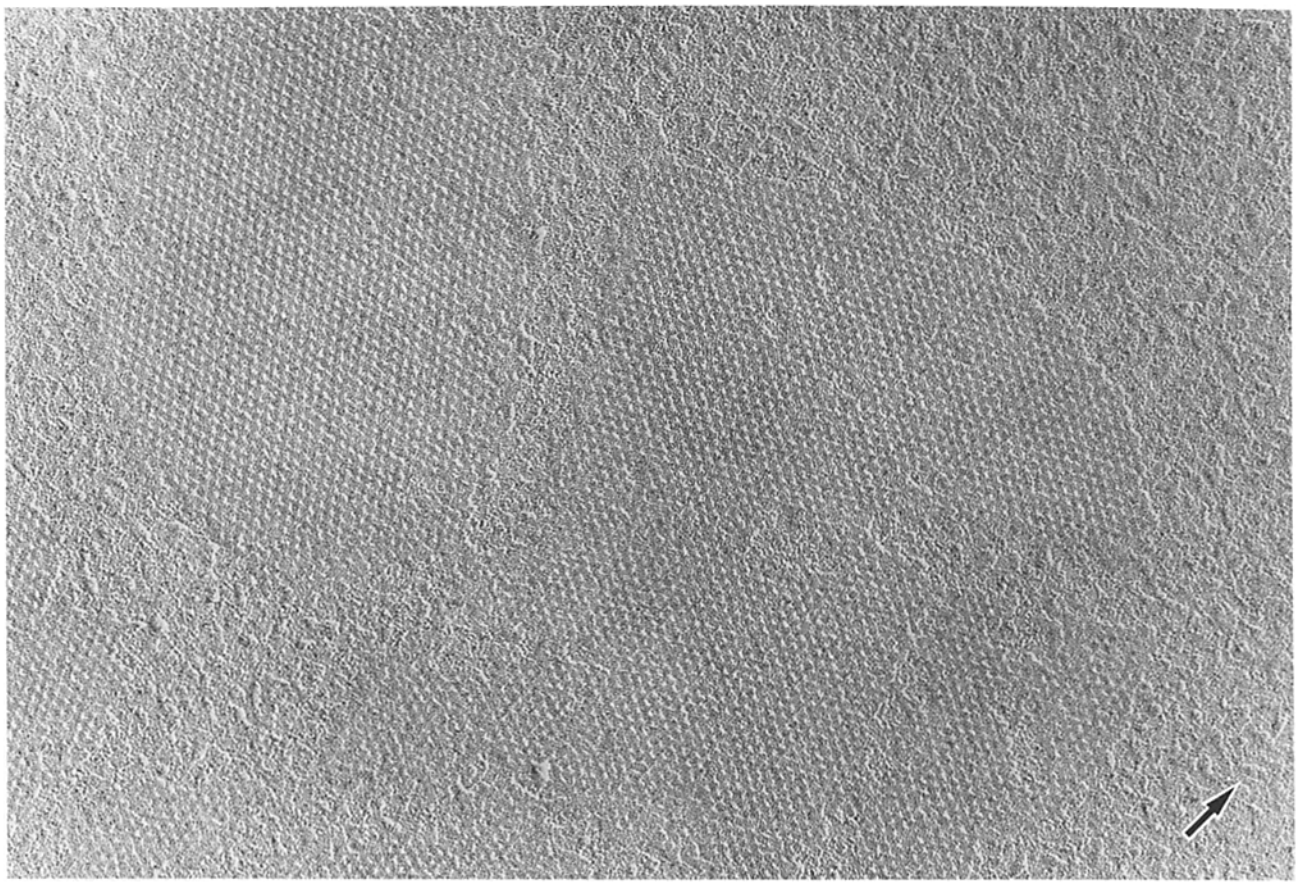

FIGURE 2 Freeze-dried crystalline sheets of LHC obtained by precipitating Triton X-100 solubilized material with $MgCl_2$ and KCl. The thickness of the membrane crystals, judging by the shadow length is 40–60 Å, indicating that they are single layers. The surface exhibits an hexagonal array of circular pits 90–100 Å diam. Only one type of surface structure was observed, suggesting that the membrane crystals were symmetrical. Shadow (white) cast in direction of arrow at an elevation angle of 45°. × 128,000.

of the same membrane crystal (Fig. 5, *c* and *d*) showed hexagonal arrays of particles measuring 80–90 Å across with one particle per crystallographic unit cell. To the limit of attainable resolution, both fracture faces were indistinguishable. This, and the fact that the two sides of the crystalline sheets showed the same surface structure, suggested that the membrane crystals were symmetrical, containing a twofold axis in the membrane plane.

The thickness of membrane crystals was measured on electron micrographs of thin sections through crystalline precipitates. Sections through stacks of several sheets were tilted so that the membrane plane was parallel to the electron beam (Fig. 6). The repeat distance in the direction perpendicular to the membrane plane was 55 Å, calibrated using the lattice constant of sheets cut parallel to the membrane plane as a standard.

Crystalline sheets of LHC negatively contrasted with uranyl acetate were easily identified at low magnification by their hexagonal outline. On the electron micrographs, the structure of negatively stained sheets appeared as a regular hexagonal mesh of stain excluding regions separated by roughly circular staining regions (Fig. 7). Thicker sheets, apparently consisting of more than one layer, with higher contrast between staining and stain-excluding regions, usually showed the same honeycomb pattern and gave sharp reflexions on a single hexagonal lattice in the optical diffractometer. This indicated that stacked layers were in register. Moiré patterns arising from sheets rotated with respect to one another were observed occasionally.

The concentration of Triton X-100 was critical for the size and order of the crystalline sheets. Good crystalline arrays were obtained with Triton X-100 concentrations ranging from 0.05 to 0.5% (wt/vol). A concentration of 0.1% (wt/vol) was used in the preparation of membrane crystals such as those seen in Fig. 7. Detergent concentrations ≥1% (wt/vol) caused the regular arrays to break up into small fragments. Such fragments are seen face-on and edge-on in Fig. 8. The strong contrast between staining and stain-excluding regions in face-on views suggested that the fragments were several layers thick with successive layers in register. In edge-on views, layers appeared as light bars against a dark background. The stacking repeat was 56–58 Å. Each fragment thus seemed to represent a minute three-dimensional crystal of LHC.

Projection Map of Negatively-Stained Membrane Crystals

Micrographs of well-ordered crystalline arrays showed diffraction patterns with spots on a hexagonal reciprocal lattice. The intensities of reflexion appeared to have 6-mm symmetry (Fig. 9). The (6,0) and (6,1) reflexions were present, indicating a resolution of 20 Å. Amplitudes and phases of reflexions were calculated by Fourier processing of selected areas. Phase origin refinements for individual images, assuming P3 or P6 symmetry, gave reproducibly lower phase residuals for P3 symmetry (see Table I). The residual of phases averaged unsymmetrized over the five best images was 20.9 for P3 and 27.8 for P6. A small increase in phase residual is expected when imposing P6 symmetry on P3 data as a result of the additional phase

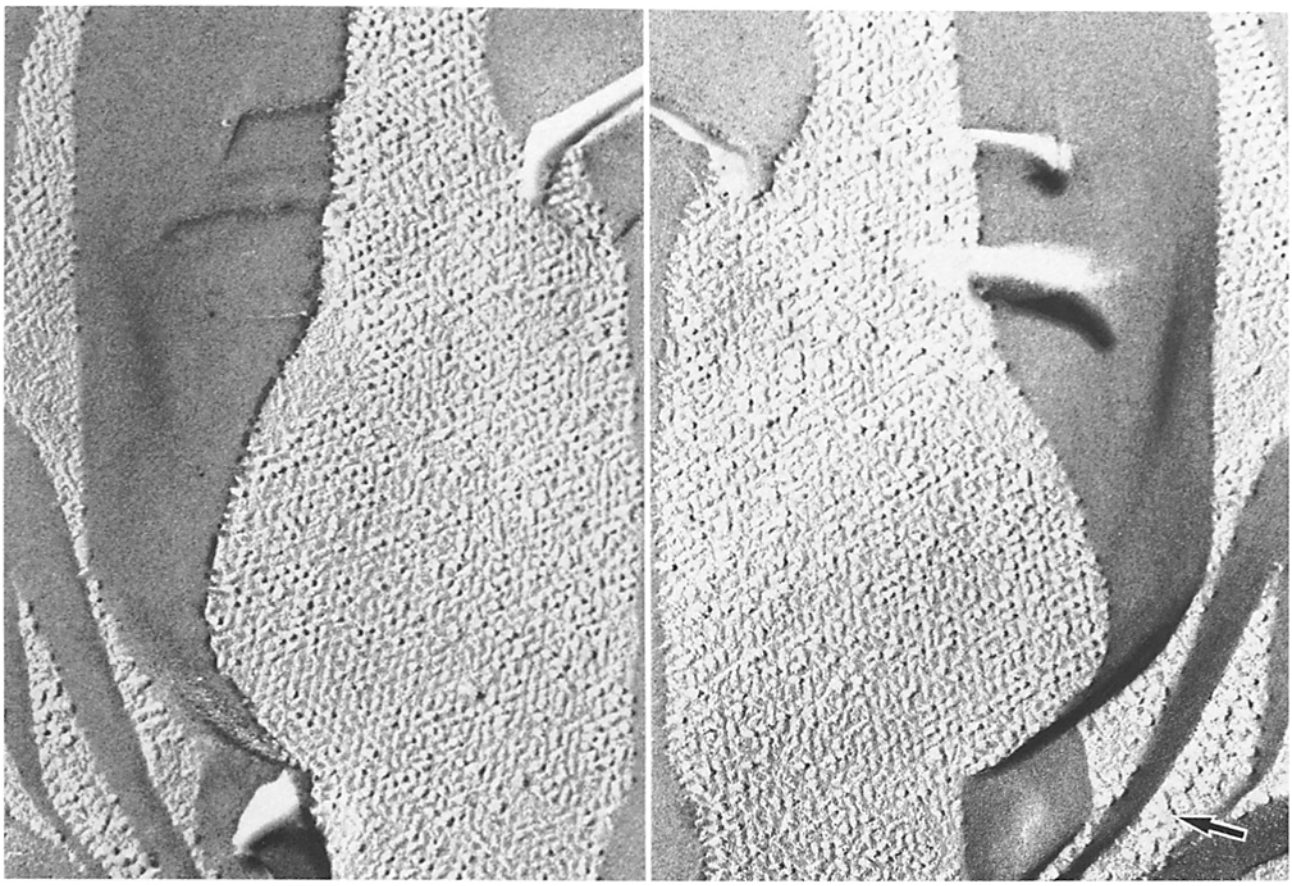

FIGURE 3 Double replica of a freeze-fractured LHC membrane crystal. The two complementary fracture faces appear to be structurally indistinguishable. Both show a hexagonal array of particles with a center-to-center distance of 125 Å. Shadow (white) cast in direction of arrow as in Fig. 2. × 124,000.

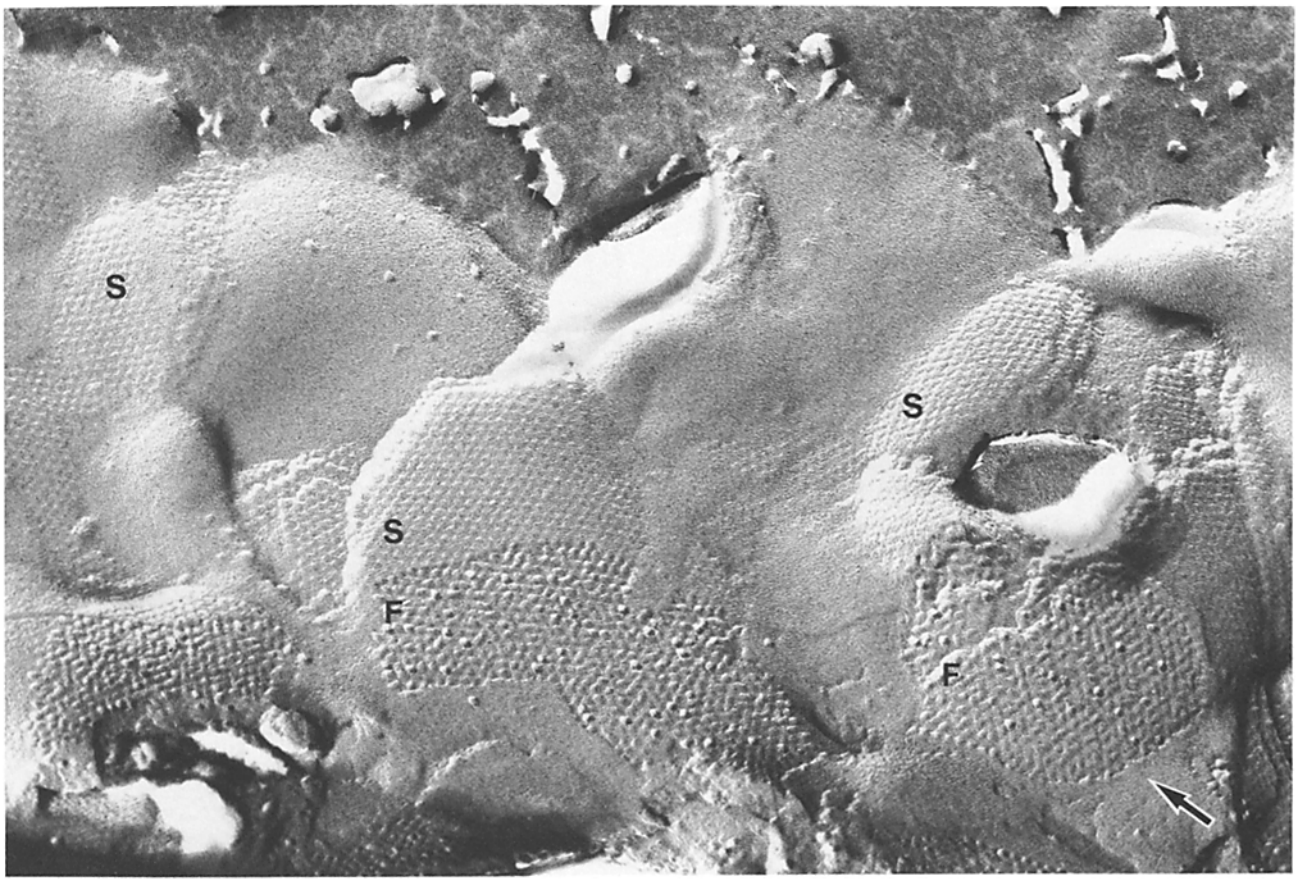

FIGURE 4 Freeze-etched LHC membrane crystals. The structure types seen on the surface (*S*) and on fracture faces (*F*) both occur in crystalline sheets where part of the top half-membrane has been removed by fracturing. Shadow (white) cast in direction of arrow as in Fig. 3. × 128,000.

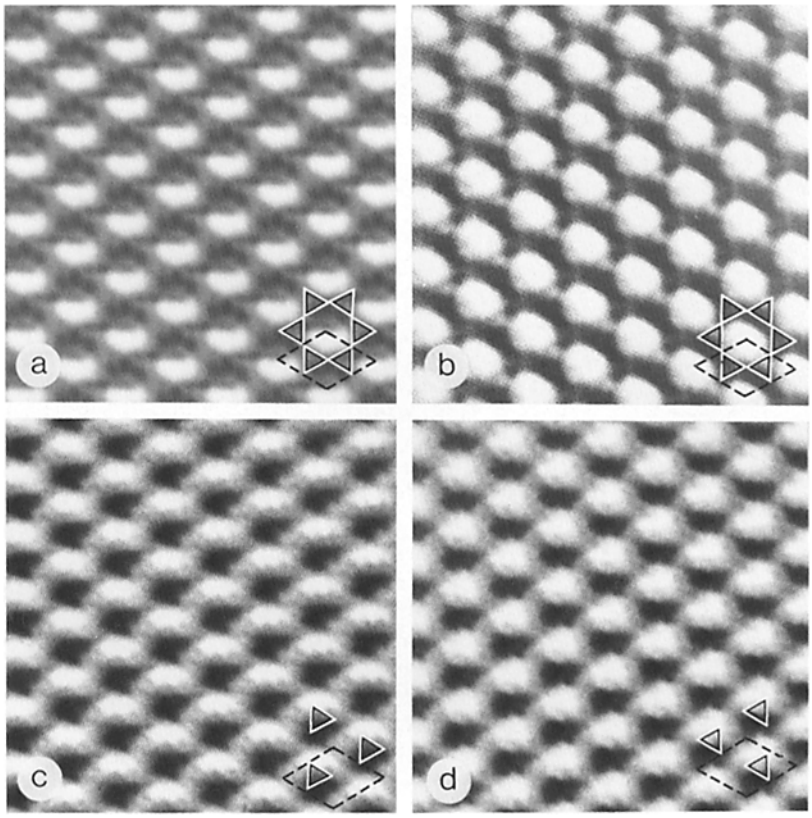

FIGURE 5 Fourier-filtered images of unidirectionally shadowed freeze-dried (*a*), freeze-etched (*b*), and freeze-fractured (*c* and *d*) LHC membrane crystals. The characteristic pattern and the crystallographic unit cell (dashed; edge = 125 Å) are outlined on each image. Shadows (cast in an upward direction) are white, as in the unfiltered images of Figs. 2–4. *a* and *b* show the surface structure of LHC membrane crystals, which is characterized by six units of triangular outline surrounding a roughly circular depression in the membrane surface. The crystallographic unit cell contains two triangular units touching at their apexes. *c* and *d* show the structure of the two complementary fracture faces of one LHC membrane crystal, both of which are characterized by hexagonal arrays of 80–90-Å particles. The crystallographic unit cell contains only one particle. Freeze-fracturing splits the membrane crystals into equal halves such that interdigitating triangular units are separated into the two half-membranes. Each particle on the fracture face therefore seems to represent one triangular unit, as indicated in the lower right-hand corner of *c* and *d*.

constraint of a twofold axis in P6 symmetry. However, comparative studies with data derived from a structure of P6 symmetry (the photosynthetic membrane of the bacterium *Rhodopseudomonas viridis*) indicated that this effect alone cannot account for the observed difference.

Amplitudes and phases, averaged over the five best images assuming P3 symmetry, are listed in Table II. Deviations of phases from P6 symmetry (where all reflexions must have phases of 0 or 180°) for strong diffraction spots such as the (1,1), (1,2), (2,1), and (2,2) reflexion were well above the mean phase error. We therefore concluded that the LHC membrane crystals had threefold rather than sixfold symmetry.

Fig. 10 is a projection map of crystalline LHC calculated from the averaged data of Table II. Maps derived from symmetrized or unsymmetrized data of individual micrographs showed the same features against a higher level of background noise. The stain-excluding material (shaded in Fig. 10) formed a hexagonal mesh apparently composed of structural units of threefold symmetry which roughly resembled equilateral triangles in projection. Within each such triangular unit three small elliptical staining regions in threefold related positions were resolved. The crystallographic unit cell contained two such elements of threefold symmetry in mirror-related positions. The near-mirror symmetry of adjacent triangular units in the projection maps, evident from their shape in outline and the position and orientation of the small elliptical staining regions, suggested a twofold axis parallel to the crystallographic *a* axis.

FIGURE 6 Thin section of crystalline precipitate of LHC fixed and dehydrated by the freeze-substitution method (30). Two stacks of five (arrow) and ten sheets are sectioned perpendicular to the membrane plane. The stacking repeat is ~55 Å. Sections were stained with lead citrate. × 130,000.

DISCUSSION

Structure and Symmetry of LHC Membrane Crystals

The surface relief of freeze-dried and freeze-etched membrane crystals of LHC revealed by image processing suggested that they were composed of structural units of roughly triangular outline in projection, arranged on a hexagonal lattice. Image analysis of negatively stained crystalline sheets confirmed this finding and revealed the shape and symmetry of the triangular units at higher resolution. A projection map indicated two structural units per crystallographic unit cell.

Complementary fracture faces of LHC membrane crystals showed the same hexagonal array of particles on both sides. The shape and size of individual particles varied somewhat, presumably due to plastic deformation (31) or decoration with ice (32). But, over a large area, the two fracture faces were indistinguishable. Image processing (Fig. 5, *c* and *d*) confirmed this finding and showed that both faces contained only one particle per crystallographic unit cell. Correlation of the structure on the fracture faces with the projection map (Fig. 10) with the structure on membrane surfaces (Fig. 5, *a* and *b*) suggested that each particle on the fracture face represented one triangular unit, so that particles from opposite half-membranes interdigitated to form a symmetrical membrane crystal. In addition to the threefold axes of symmetry perpendicular to the membrane plane, crystalline sheets of LHC therefore seemed to contain a twofold symmetry axis in the membrane plane.

Two other, independent, lines of evidence suggested such a twofold axis: (*a*) the two surfaces of membrane crystals were indistinguishable in metal-shadowed, freeze-dried and freeze-etched sheets at a resolution of ~30 Å; and (*b*) in the contour map (Fig. 10), adjacent triangular units appeared to be mirror symmetric in projection, apart from minor differences that could be accounted for by uneven staining (33). Since mirror symmetry of molecules does not occur in biological systems, this would indicate that adjacent triangular units are related by a twofold axis in the membrane plane.

The direction of the twofold axis, as indicated by the projection map, is parallel to the unit cell edge (Fig. 10). The resulting space group thus appears to be P321. This is corroborated by the observed phases of reflexions. In the P321 space group, axial reflexions (h,0) should have phases of 0 or 180°. Table II shows that deviations of axial reflexions from these values are within the average mean phase error, whereas nonaxial reflexions deviate by up to 60°.

Li and Hollingshead, judging from the 6-mm symmetry of reflexion intensities in the low resolution optical diffraction pattern of negatively stained material, proposed that the space group of LHC membrane crystals was P622. A correct assignment of space group requires, however, the analysis of reflexion phases, because two other space groups, P321 and P312, also give rise to diffraction intensities of 6-mm symmetry in projection. A comparison of phase residuals calculated assuming sixfold and threefold symmetry certainly points to the P321 space group. P622 seems unlikely for another reason. In this space group, each triangular unit would contain a twofold axis of symmetry parallel to the membrane plane. The two sides exposed by one triangular unit on the two membrane surfaces would therefore be equivalent and equally anchored in the two half-membranes. When freeze-fracturing a membrane crystal composed of such hypothetical "dimers," one would expect a

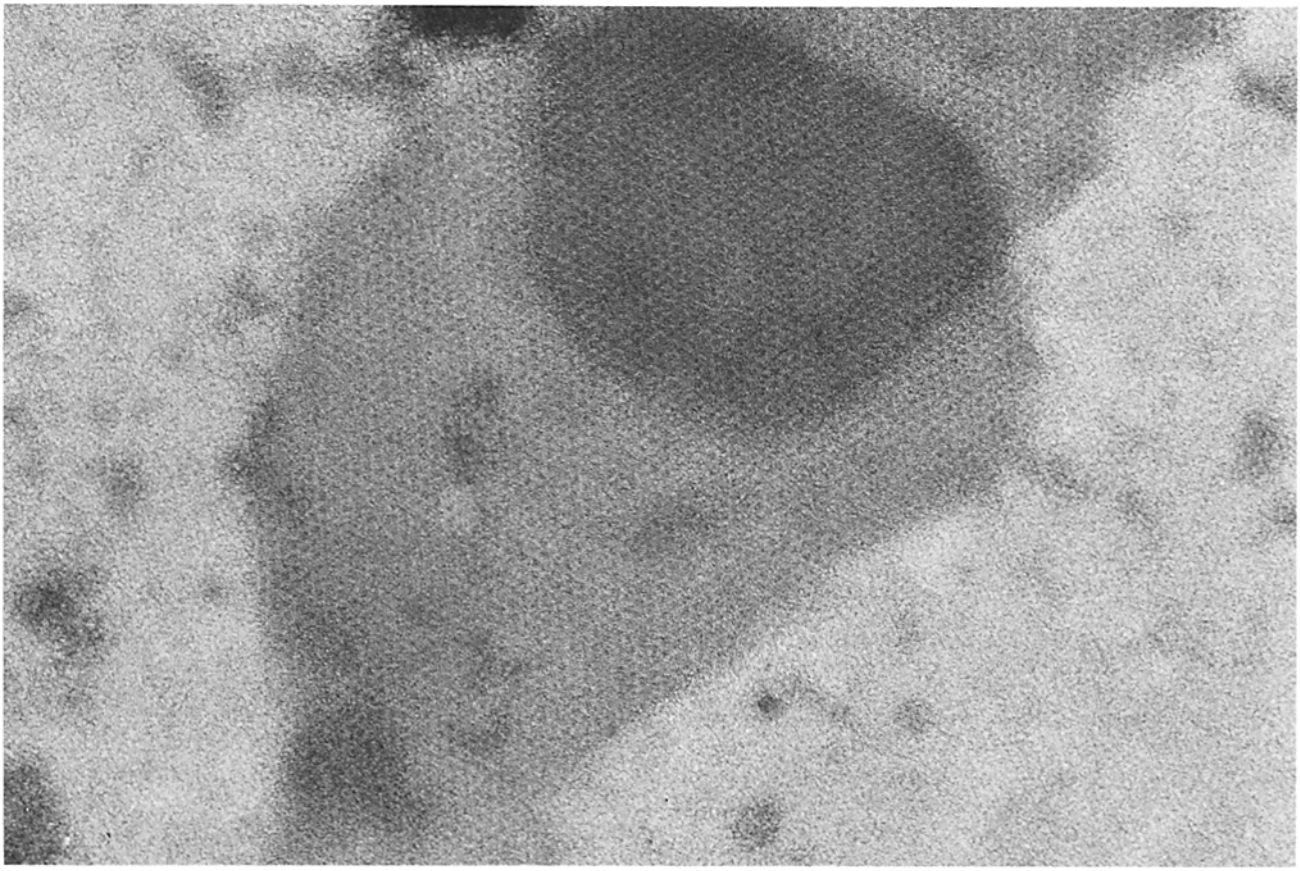

FIGURE 7 Membrane crystals of LHC negatively stained with uranyl acetate. The crystals were prepared at pH 6.8 in 10 mM $MgCl_2$, 200 mM KCl, and a Triton X-100 concentration of 0.1% (wt/vol). Stain-excluding regions form an hexagonal mesh. The lattices of overlapping sheets (darker area) are in register. × 136,000.

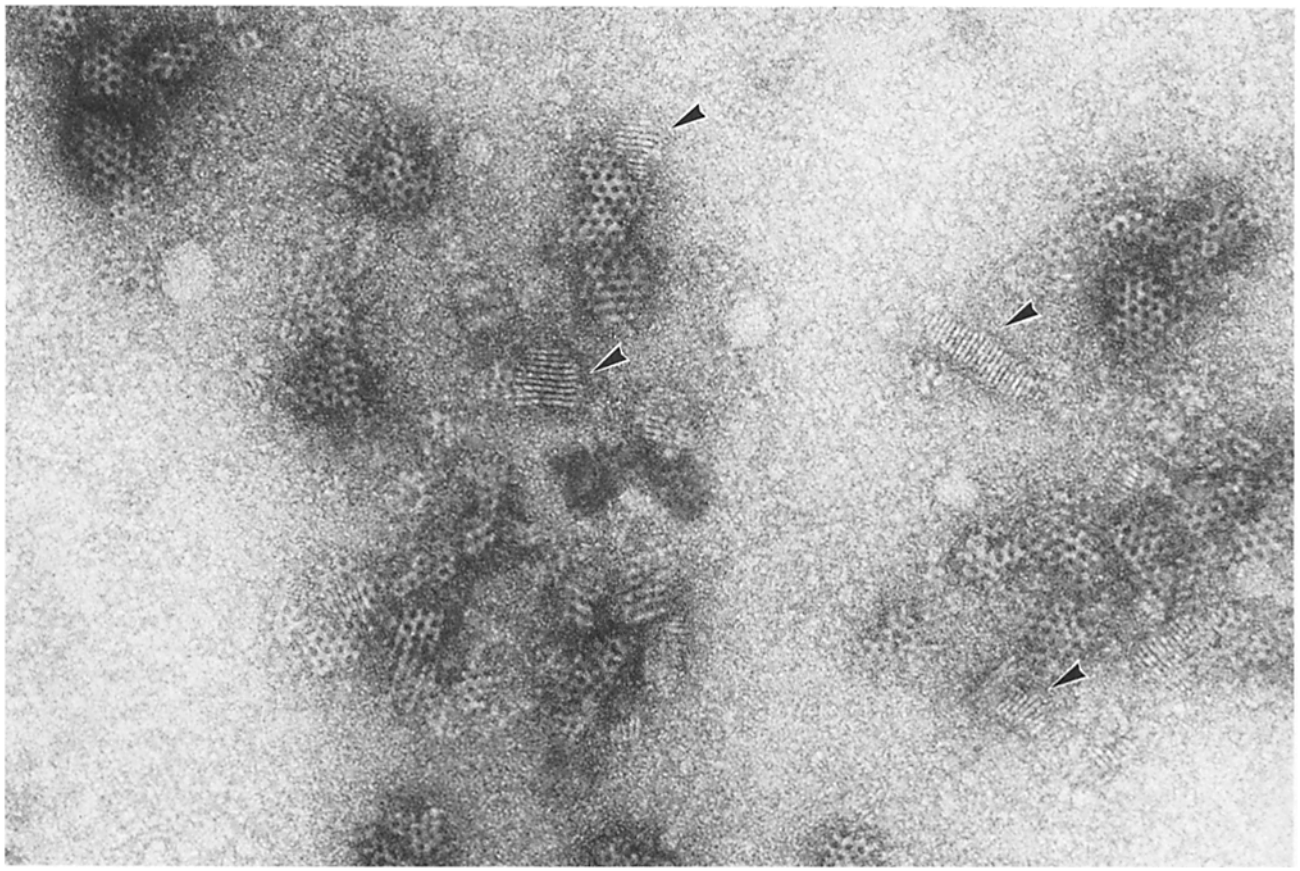

FIGURE 8 Negatively stained fragments of LHC crystals that formed in the presence of Triton X-100 concentrations of ~1% (wt/vol). Edge-on views (arrowheads) show stacks of up to 20 layers with a repeat distance of 56–58 Å. The honeycomb structure of fragments seen face-on indicates that successive layers are in register. × 140,000.

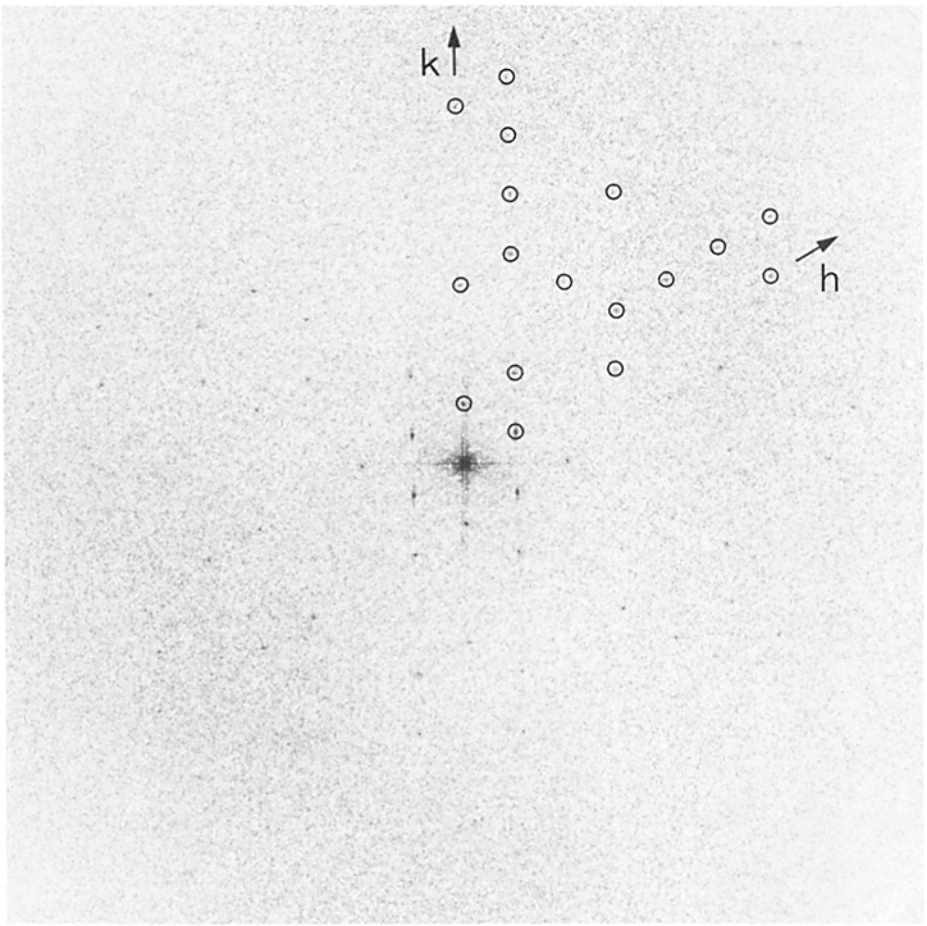

FIGURE 9 Computer generated diffraction pattern of a negatively stained LHC membrane crystal. *h* and *k* are the reciprocal lattice vectors. The reflexion intensities have 6-mm symmetry. Reflexions out to the (6,0) and (6,1) reflexion are observed. An analysis of the relationships between phases of reflexions indicated threefold rather than sixfold symmetry for the membrane crystals in projection.

TABLE I

Phase Residuals of Five Individual Images and Their Average

Image No.	P3 phase residual	P6 phase residual	No. of independent reflexions
	degrees	*degrees*	
1	18.02	28.00	20
2	17.92	21.81	19
3	21.91	26.91	17
4	17.18	34.04	15
5	20.07	28.78	14
Avg	20.9	27.8	26

TABLE II

Average Reflexion Amplitudes and Phases

h	k	Amplitude	Phase	h	k	Amplitude	Phase
			degrees				*degrees*
1	0	1,000	175	2	2	141	312
2	0	194	359	3	2	102	351
3	0	273	184	4	2	110	6
4	0	136	13	5	2	126	179
5	0	156	184	1	3	305	176
6	0	171	170	2	3	124	29
1	1	575	24	3	3	154	185
2	1	182	221	1	4	210	346
3	1	319	165	2	4	93	347
4	1	186	350	3	4	104	334
5	1	126	120	1	5	119	152
6	1	103	354	2	5	77	216
1	2	182	151	1	6	116	342

random distribution of structural units into the two half-membranes, with two particles per crystallographic unit cell in averaged images. This conflicts with our experimental result.

Fig. 11 is a schematic drawing of the structure as it appears from our data. The crystallographic unit cell contains two structural units of threefold symmetry and opposite handedness in projection. The triangular units are shown protruding by different amounts on either side of the membrane sheet to emphasize the fact that individual units are not symmetrical with respect to the membrane plane. Adjacent triangular units are related by a twofold axis so that they alternate in orientation perpendicular to the membrane. The two membrane surfaces therefore are indistinguishable. When an LHC membrane crystal is fractured, structural units of one orientation go into one half-membrane whereas those of opposite orientation remain in the other half-membrane, thus generating two equal halves with one particle per crystallographic unit cell.

Membrane crystals of LHC have a tendency to form stacks, reflecting the function of LHC as a membrane adhesion factor. In our investigations of the structure of negatively stained membrane crystals we restricted our analysis to the thinnest sheets (judged by their optical density on the negative), which we assumed to be single layers. Fig. 2 demonstrates that single layers do occur; they are, however, much less abundant than stacked sheets. Image analysis of regions where two thin membrane crystals overlap (as in Fig. 7) showed the same features as thinner sheets, including the apparent mirror symmetry of adjacent triangular units in the projection map. Therefore, the

number of layers in a sheet did not seem to be critical to the observed structure and symmetry in projection.

Other reports on the structure of freeze-fractured and freeze-etched crystalline LHC precipitates agree with our findings. Hexagonal arrays of particles on fracture faces have been described for preparations of pea (13, 14, 17, 21), spinach (7, 37), and barley LHC (18). The formation of crystalline arrays of LHC thus seems to be a property common to widely different species of plants.

Symmetry and Composition of the Light-harvesting Complex

Crystalline precipitates of LHC contained two polypeptides of 25,000 and 27,000 mol wt. These polypeptides were apparently identical to those isolated by Bennet from SDS-solubilized pea thylakoids that were both phosphorylated (15) and showed extensive structural homology (16).

Fracture faces of native, stacked thylakoids from grana regions contain large numbers of particles similar in shape and size to those found on fracture faces of crystalline LHC (34). The absence of such particles from freeze-fracture thylakoids of LHC-deficient mutants (18) implied that they represent the light-harvesting complex. Assuming that the complex does not rearrange during isolation, it seems reasonable to conclude that each triangular unit seen on the membrane surface and in the projection map is one light-harvesting complex, as it occurs in the thylakoid membrane. Biochemical analysis of undenatured LHC has shown that the native complex is an oligomer (7, 10, 14, 23). The apparent molecular weight of the oligomeric complex (LHCP[1]) on nondenaturing gels has been variously given as 67,000 (9), 68,000 (10), 80,000 (14, 16), and 60,000–100,000 (3). These values seem to suggest that the oligomer contains three to four polypeptides of 23,000 to 27,000 mol wt. However, as Thornber (1) points out, the molecular weight of protein-chlorophyll complexes may be underestimated by this method.

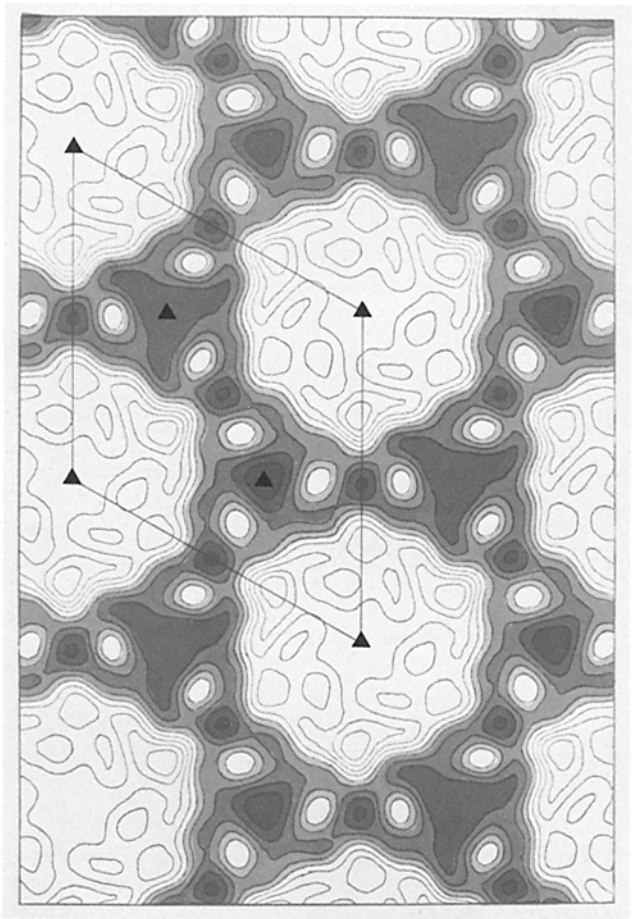

FIGURE 10 Projection map of negatively stained LHC membrane crystals, calculated from averaged data of Table II. Stain-excluding regions are shown in shades of gray. The crystallographic unit cell contains two structural units of threefold symmetry. Within each triangular unit three elliptical staining regions are resolved. The stain distribution in the unit cell suggests that the two triangular units are mirror-symmetric in projection. Deviation from mirror symmetry, evident in the contours of the upper three gray levels, could be due to uneven staining of the two membrane surfaces (33). The mirror symmetry of the projection map implies a twofold axis in the membrane plane along the edge of the crystallographic unit cell.

We estimated the volume of a structural unit of threefold symmetry (such as drawn in Fig. 11) from its area in projection and the thickness of membrane crystals, and compared the value with the molecular volume of bacteriorhodopsin, obtained in the same way from its area in projection (35) and the thickness of purple membrane (36). Assuming that the LHC protein has the same density as bacteriorhodopsin, the molecular weight of one such unit would be ~170,000. This value is somewhat lower than the estimate of McDonnel and Staehelin (202,000–234,000 mol wt; [14]) based on the size of particles on the fracture face that may have included some adhering lipid or detergent. If our estimate of the mass of one unit of threefold symmetry is correct, and if the whole estimated volume is taken up by protein, three polypeptides each of 25,000 and 27,000 mol wt could be accommodated per triangular unit. The threefold symmetry of the structural unit implies that it is composed of three identical subunits. These subunits may correspond to the monomeric LHC that seems to be a hetero-dimer of the two polypeptides. Results of the biochemical analysis that indicated that the monomeric complex contains both polypeptides support this model.

Effect of Detergent Concentration on the Structure of Membrane Crystals

Apart from the pH and the concentration of $MgCl_2$ and KCl, the concentration of the detergent, Triton X-100, was critical to the appearance and degree of order of LHC membrane crystals. Removal of the detergent caused an almost complete loss of order in the membrane plane, as revealed by freeze-fracturing that showed warped, closely stacked sheets similar to those reported by Li and Hollingshead (21) had formed in the absence of lipid. The best LHC membrane crystals we found formed in the presence of Triton X-100 concentrations ~0.1% (wt/vol). Triton X-100 concentrations >0.5% (wt/vol) caused increasing fragmentation of membrane crystals. Excess detergent appeared to weaken interactions between complexes in the membrane plane, presumably owing to Triton molecules inserting themselves between the triangular units. LHC complexes interacting in a direction perpendicular to the membrane plane were not affected by the detergent. This is demonstrated by Fig. 8 in which small fragments of membrane crystals form extensive stacks at Triton concentrations that disrupt interactions in the membrane plane.

With one exception, the material used in various laboratories to obtain crystalline arrays of LHC was isolated from Triton X-100-solubilized thylakoids. Siegel et al. (37) produced hex-

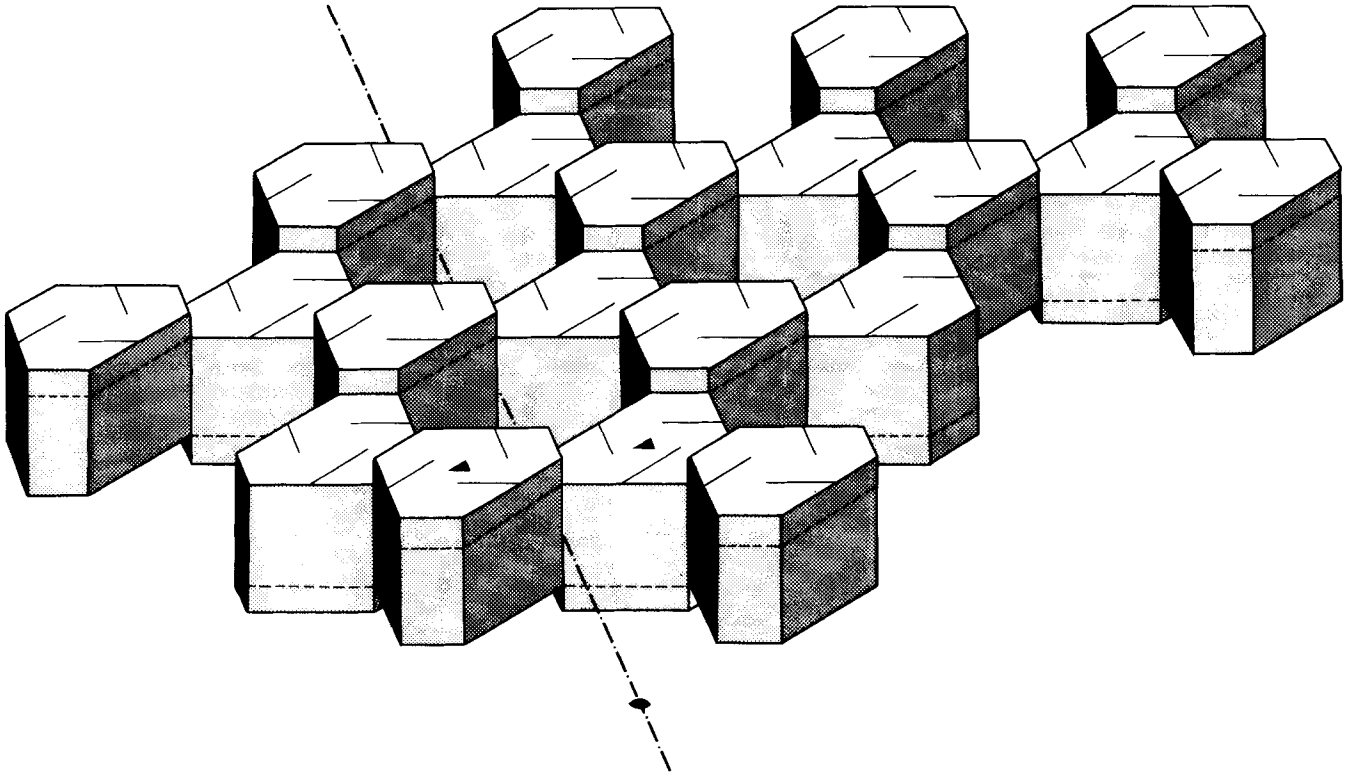

FIGURE 11 Schematic drawing of the structure of LHC membrane crystals as it appears from Fourier-filtered images of freeze-dried, freeze-etched, and freeze-fractured membrane crystals (Fig. 5), and the projection map (Fig. 10). Adjacent units of threefold symmetry are related by a twofold symmetry axis in the membrane plane (dash-dotted line). In projection they therefore appear mirror-symmetric with respect to one another. Freeze-fracturing separates units of equal orientation into two equal half-membranes.

agonal arrays of a very similar structure by merely adding lipid to spinach thylakoids. We were able to reproduce this experiment with pea thylakoids. Freeze-dried and freeze-fractured lipid vesicles fused with thylakoid membranes were structurally identical to the arrays formed by precipitation of the Triton X-100 solubilized fraction. LHC that has not been exposed to detergent thus can form the same crystalline arrays as detergent-treated material, suggesting that Triton X-100 does not disrupt the native structure of the complex. This is also suggested by results of spectroscopic investigations (38) that indicated that the native orientation of LHC pigments is preserved in the Triton X-100 solubilized complex.

Hexagonal arrays have so far not been described in thylakoids of higher plants, although orthogonal and square arrays do occur (39–41). The asymmetry of LHC in the thylakoid membrane, apparently due to unidirectional insertion of the complex, has been demonstrated (8). It appears that for the formation of regular arrays, bidirectional, symmetrical insertion of the complex into the reconstituted membrane is essential. When the natural asymmetry of the membrane is lost, either through an excess of lipid or solubilization with detergent, LHC has a pronounced tendency to form hexagonal crystalline arrays.

We would like to thank Professor O. Kübler for the use of image processing facilities and Professor K. Mühlethaler for critical reading of the manuscript.

W. Kühlbrandt acknowledges financial support from the Roche Research Foundation.

Received for publication 21 September 1982, and in revised form 28 January 1983.

REFERENCES

1. Thornber, J. P. 1975. Chlorophyll-proteins: light-harvesting and reaction center components of plants. *Annu. Rev. Plant Physiol.* 26:127–158.
2. Thornber, J. P., and J. Barber. 1979. Photosynthetic pigments and models for their organization *in vivo*. *In* Photosynthesis in Relation to Model Systems. J. Barber, editor. Elsevier/North Holland Biomedical Press, Amsterdam. 27–70.
3. Thornber J. P., J. P. Markwell, and S. Reinman. 1979. Plant chlorophyll-protein complexes: recent advances. *Photochem. Photobiol.* 29:1205–1216.
4. Bennet, J. 1979. The protein that harvests sunlight. *Trends Biochem. Sci.* 4:268–271.
5. Andersson, B., and J. M. Anderson. 1980. Lateral heterogeneity in the distribution of chlorophyll-protein complexes of the thylakoid membranes of spinach chloroplasts. *Biochim. Biophys. Acta.* 593:427–440.
6. Takahashi, M., and E. L. Gross. 1978. Use of immobilised light-harvesting chlorophyll a/b-protein to study the stoichiometry of self-association. *Biochemistry.* 17:806–810.
7. Ryrie, I. J., J. M. Anderson, and D. J. Goodchild. 1980. The role of the light-harvesting chlorophyll a/b-protein complex in chloroplast membrane stacking. *Eur. J. Biochem.* 107:345–354.
8. Andersson, B., J. M. Anderson, and I. J. Ryrie. 1982. Transbilayer organization of the chlorophyll-proteins of spinach thylakoids. *Eur. J. Biochem.* 123:465–472.
9. Apel, K. 1977. The light-harvesting chlorophyll a/b-protein complex of the green alga *Acetabularia mediterranea*. Isolation and characterization of two subunits. *Biochim. Biophys. Acta.* 462:390–402.
10. Dunkley, P. R., and J. M. Anderson. 1979. The light-harvesting chlorophyll a/b-protein complex from barley thylakoid membranes. Polypeptide composition and characterization of an oligomer. *Biochim. Biophys. Acta.* 545:174–187.
11. Ryrie, I. J., and N. Fuad. 1982. Membrane adhesion in reconstituted proteoliposomes containing the light-harvesting chlorophyll a/b-protein complex: the role of charged surface groups. *Arch. Biochem. Biophys.* 214:475–488.
12. Burke, J. J., C. L. Ditto, and C. J. Arntzen. 1978. Involvement of the light-harvesting complex in cation regulation of excitation energy distribution in chloroplasts. *Arch. Biochem. Biophys.* 187:252–263.
13. Mullet, J. E., and C. J. Arntzen. 1980. Simulation of grana stacking in a model membrane system. Mediation by a purified light-harvesting pigment-protein complex from chloroplasts. *Biochim. Biophys. Acta.* 589:100–117.
14. McDonnel, A., and L. A. Staehelin. 1980. Adhesion between liposomes mediated by the chlorophyll a/b light-harvesting complex isolated from chloroplast membranes. *J. Cell Biol.* 84:40–56.
15. Bennet, J. 1979. Chloroplast phosphoproteins. Phosphorylation of polypeptides of the light-harvesting chlorophyll-protein complex. *Eur. J. Biochem.* 99:133–137.
16. Bennet, J., J. P. Markwell, M. P. Skrdla, and J. P. Thornber. 1981. Higher plant chlorophyll a/b-protein complexes: studies on the phosphorylated apoproteins. *FEBS (Fed. Eur. Biochem. Soc.) Lett.* 131:325–330.
17. Steinback, K. E., J. J. Burke, J. E. Mullet, and C. J. Arntzen. 1978. The role of the light-harvesting complex in cation-mediated grana formation. *In* Chloroplast Development. G. Akoyunoglou, and J. H. Argyroudi-Akoyunoglou, editors. Elsevier/North Holland

Biomedical Press, Amsterdam. 389–400.
18. Simpson, D. J. 1979. Freeze-fracture studies on barley plastid membranes. III. Location of the light-harvesting chlorophyll-protein. *Carlsberg Res. Commun.* 44:305–336.
19. Izawa, S., and N. E. Good. 1966. Effects of salt and electron transport on the conformation of isolated chloroplasts. II. Electron microscopy. *Plant Physiol. (Bethesda).* 41:544–553.
20. Arntzen, C. J., and J. J. Burke. 1980. Analysis of dynamic changes in membrane architecture: electron microscopic approach. *Methods Enzymol.* 69:520–538.
21. Li, J., and C. Hollingshead. 1982. Formation of crystalline arrays of chlorophyll *a/b*-light-harvesting protein by membrane reconstitution. *Biophys. J.* 37:363–370.
22. Anderson, J. M., J. C. Waldron, and S. W. Thorne. 1978. Chlorophyll-protein complexes of spinach and barley thylakoids. *FEBS (Fed. Eur. Biochem. Soc.) Lett.* 92:227–233.
23. Anderson, J. M. 1980. P-700 content and polypeptide profile of chlorophyll-protein complexes of spinach and barley thylakoids. *Biochim. Biophys. Acta.* 591:113–126.
24. Takács, B. 1979. Electrophoresis of proteins in polyacrylamide slab gels. *In* Immunological Methods. I. Lefkovits and B. Pernis, editors. Academic Press, New York. 81–105.
25. Wray, W., T. Boulikas, V. P. Wray, and R. Hancock. 1981. Silver staining of proteins in polyacrylamide gels. *Anal. Biochem.* 118:197–203.
26. Arnon, D. I. 1949. Copper enzymes in isolated chloroplasts. Polyphenol-oxidase in *Beta vulgaris. Plant Physiol. (Bethesda).* 24:1–10.
27. Lowry, O. H., N. J. Rosebrough, A. L. Farr, and R. J. Randall. 1951. Protein measurement with the folin phenol reagent. *J. Biol. Chem.* 193:265–275.
28. Dulley, J. R., and P. A. Grieve. 1975. A simple technique for eliminating interference by detergent in the Lowry method of protein determination. *Anal. Biochem.* 64:136–141.
29. Mühlethaler, K., E. Wehrli, and H. Moor. 1970. Double fracturing methods for freeze-etching. *Proc. 7th Int. Congr. Electron Microsc. (Grenoble).* 1:449–450.
30. Müller, M., T. Marti, and S. Kriz. 1980. Improved structural preservation by freeze-substitution. *Proc. 7th Eur. Congr. Electron Microsc. (Den Haag).* 720–721.
31. Sleytr, U. B., and A. W. Robards. 1982. Understanding the artefact problem in freeze-fracture replication: a review. *J. Microsc. (Oxf.).* 126:107–122.
32. Walzthöny, D., H. Moor, and H. Gross. 1981. Ice crystals specifically decorate hydrophilic sites on freeze-fractured model membranes. *Ultramicroscopy.* 6:259–266.
33. Unwin, P. N. T., and G. Zampighi. 1980. Structure of the junction between communicating cells. *Nature (Lond.).* 283:545–549.
34. Goodenough, U. W., and L. A. Staehelin. 1971. Structural differentiation of stacked and unstacked chloroplast membranes. Freeze-etch electron microscopy of wild-type and mutant strains of *Chlamydomonas. J. Cell Biol.* 48:594–619.
35. Unwin, P. N. T., and R. Henderson. 1975. Molecular structure determination by electron microscopy of unstained crystalline specimens. *J. Mol. Biol.* 94:425–440.
36. Henderson, R. 1975. The structure of purple membrane from *Halobacterium halobium.* Analysis of x-ray diffraction patterns. *J. Mol. Biol.* 93:123–138.
37. Siegel, C. O., A. E. Jordan, and K. R. Miller. 1981. Addition of lipid to the photosynthetic membrane: effect on membrane structure and energy transfer. *J. Cell Biol.* 91:113–125.
38. Haworth, D., C. J. Arntzen, P. Tapie, and J. Breton. 1982. Orientation of pigments in the thylakoid membrane and in the isolated chlorophyll-protein complexes of higher plants. I. Determination of optimal conditions for linear dichroism measurement. *Biochim. Biophys. Acta.* 679:428–435.
39. Staehelin, L. A. 1975. Chloroplast membrane structure: intramembranous particles of different size make contact in stacked membrane regions. *Biochim. Biophys. Acta.* 408:1–11.
40. Staehelin, L. A. 1976. Reversible particle movements associated with unstacking and restacking of chloroplast membranes in vitro. *J. Cell Biol.* 71:136–158.
41. Miller, K. R., G. J. Miller, and K. R. McIntyre. 1976. The light-harvesting chlorophyll-protein complex of photosystem II. Its location in the photosynthetic membrane. *J. Cell Biol.* 71:624–638.